

# Self-Calibrating TPOS Gear Tooth Sensor Optimized for Automotive Cam Sensing Applications

## Features and Benefits

- Tight timing accuracy over operating temperature range
- True zero-speed operation
- TPOS (True Power-On State)
- Air-gap-independent switchpoints
- High immunity to vibration
- Large operating air gaps
- Operation with supply voltages down to 3.3 V
- Digital output representing target profile
- Single-chip solution for high reliability
- Optimized Hall IC/magnet system

Continued on the next page...

## Packages: 4 pin SIP (suffix SE)



Not to scale

## Description

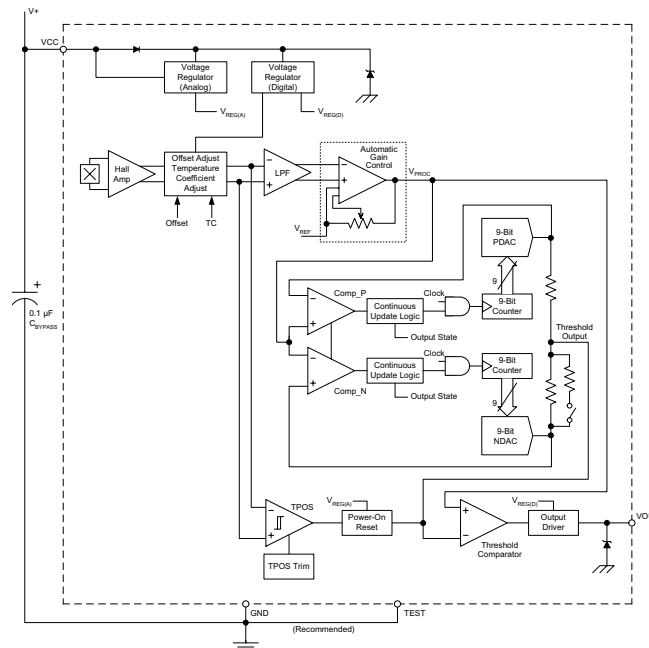
Recognizing the increasingly stringent requirements for EMC/EMI in automotive applications, Allegro has taken the necessary steps to design devices that are capable of withstanding the effects of radiated and conducted transients. The ATS673 and ATS674 devices have been designed specifically for this purpose. Advanced circuitry on the die allows them to survive positive and negative transient pulses on both the input and output.

The ATS673 and ATS674 devices retain all of the same characteristics as the ATS671 and ATS672. The devices remain true zero-speed gear tooth sensors with optimized Hall IC/magnet configuration in an SIP (single in-line package). The SIP assembly consists of a molded package that holds together a samarium cobalt magnet, a pole piece, and a true zero-speed Hall IC that has been optimized to the magnetic circuit.

The sensor incorporates a single element Hall IC that switches in response to magnetic signals created by a ferrous target. The IC contains a sophisticated digital circuit designed to eliminate the detrimental effects of magnet and system offsets. Signal processing is used to provide zero-speed

Continued on the next page...

## Functional Block Diagram



# ATS673 and ATS674

# Self-Calibrating TPOS Gear Tooth Sensor Optimized for Automotive Cam Sensing Applications

## Features and Benefits (continued)

- AGC and reference adjust circuit
- Undervoltage lockout

## Description (continued)

performance independent of air gap and also to dynamically adapt device performance to the typical operating conditions found in automotive applications, particularly cam sensing applications (reduced vibration sensitivity).

High-resolution (9-bit) peak detecting DACs are used to set the adaptive switching thresholds of the devices, ensuring high accuracy

even in the presence of gear eccentricity. Hysteresis in the thresholds reduces the negative effects of anomalies in the magnetic signal (such as magnetic overshoot) associated with the targets used in many automotive applications. The ATS673 and 674 also include a low bandwidth filter that increases the noise immunity and the signal to noise ratio of the sensor.

Two options are available for output polarity, low over tooth (LT) and high over tooth (HT). For applications requiring absolute accuracy use the ATS674. The ATS673 should be used for targets with high wobble.

## Selection Guide

Part Number	Pb-free <sup>1</sup>	V <sub>OUT</sub> (Over Tooth)	Application	Packing <sup>2</sup>
ATS673LSETN-LT-T	Yes	Low	High target wobble	13-in. reel, 450 pieces/reel
ATS673LSETN-HT-T	Yes	High		
ATS674LSETN-LT-T	Yes	Low	High absolute edge detection accuracy	
ATS674LSETN-HT-T	Yes	High		

<sup>1</sup>Pb-based variants are being phased out of the product line. Certain variants cited in this footnote are in production but have been determined to be NOT FOR NEW DESIGN. This classification indicates that sale of this device is currently restricted to existing customer applications. The device should not be purchased for new design applications because obsolescence in the near future is probable. Samples are no longer available. Status change: May 1, 2006. These variants include: ATS673LSETN-LT, ATS673LSETN-HT, ATS674LSETN-LT, and ATS674LSETN-HT.

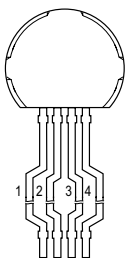
<sup>2</sup>Contact Allegro for additional packing options.

## Absolute Maximum Ratings

Characteristic	Symbol	Notes	Rating	Units
Supply Voltage	V <sub>CC</sub>		28	V
Reverse-Supply Voltage	V <sub>RCC</sub>		-18	V
Continuous Output Current	I <sub>OUT</sub>		20	mA
Reverse Output Current	I <sub>ROUT</sub>		50	mA
Operating Ambient Temperature	T <sub>A</sub>	Range L	-40 to 150	°C
Maximum Junction Temperature	T <sub>J(max)</sub>		165	°C
Storage Temperature	T <sub>stg</sub>		-65 to 170	°C



## Pin-out Diagram



## Terminal List

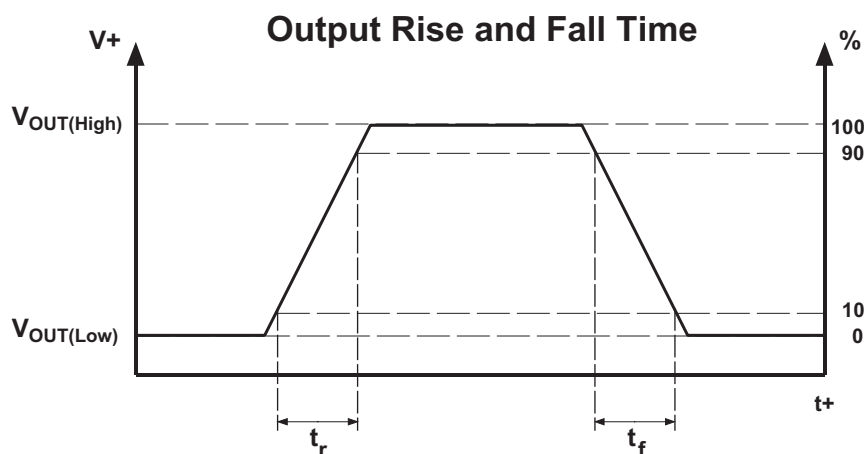
Name	Description	Number
VCC	Connects power supply to chip	1
VOUT	Device output	2
TEST	For Allegro use, float or tie to GND	3
GND	Ground terminal	4



**OPERATING CHARACTERISTICS** Valid at  $T_A = -40^{\circ}\text{C}$  to  $150^{\circ}\text{C}$ ,  $T_J \leq T_{J(\text{max})}$ , over full range of AG, unless otherwise noted

Characteristic	Symbol	Test Conditions	Min.	Typ. <sup>1</sup>	Max.	Units	
<b>ELECTRICAL CHARACTERISTICS</b>							
Supply Voltage	$V_{CC}$	Operating; $T_J < T_{J(\text{Max})}$	3.3	–	26.5	V	
Undervoltage Lockout	$V_{CCUV}$		–	–	$<V_{CC(\text{Min})}$	V	
Supply Zener Clamp Voltage	$V_{Z\text{Supply}}$	$I_{CC} = I_{CC(\text{Max})} + 3 \text{ mA}$ , $T_A = 25^{\circ}\text{C}$	28	31	35	V	
Supply Zener Current <sup>2</sup>	$I_{Z\text{Supply}}$	$V_{\text{Supply}} = 27 \text{ V}$	–	–	14	mA	
Supply Current	$I_{CC}$	Output = OFF or ON	3	6.5	11	mA	
Reverse Supply Current	$I_{RCC}$	$V_{RCC} = -18 \text{ V}$	–	-5	-10	mA	
<b>POWER-ON CHARACTERISTICS</b>							
Power-On Time <sup>3</sup>	$t_{PO}$	Gear Speed $< 100 \text{ rpm}$ ; $V_{CC} > V_{CC(\text{Min})}$	–	–	500	$\mu\text{s}$	
<b>OUTPUT CHARACTERISTICS</b>							
Low Output Voltage	$V_{\text{OUT}(\text{Sat})}$	$I_{\text{SINK}} = 15 \text{ mA}$ , Output = ON	–	200	450	mV	
Output Zener Voltage	$V_{Z\text{OUT}}$	$I_{\text{OUT}} = 3 \text{ mA}$ , $T_A = 25^{\circ}\text{C}$	30	–	–	V	
Output Current Limit	$I_{\text{OUTLIM}}$	Output = ON, $V_{\text{OUT}} = 12 \text{ V}$	35	57	90	mA	
Output Leakage Current	$I_{\text{OUTOFF}}$	Output = OFF, $V_{\text{OUT}} = V_{CC(\text{Max})}$	–	–	10	$\mu\text{A}$	
Output Rise Time	$t_r$	10/90% points; $R_{\text{LOAD}} = 500 \Omega$ , $C_{\text{LOAD}} = 10 \text{ pF}$ , $T_A = 25^{\circ}\text{C}$	–	0.9	5	$\mu\text{s}$	
Output Fall Time	$t_f$	10/90% points; $R_{\text{LOAD}} = 500 \Omega$ , $C_{\text{LOAD}} = 10 \text{ pF}$ , $T_A = 25^{\circ}\text{C}$	–	0.5	5	$\mu\text{s}$	
Output Polarity	$V_{\text{OUT}}$	HT device option	Over tooth	–	HIGH	–	V
			Over valley	–	LOW	–	V
		LT device option	Over tooth	–	LOW	–	V
			Over valley	–	HIGH	–	V

Continued on the next page...



**OPERATING CHARACTERISTICS, continued** Valid at  $T_A = -40^\circ\text{C}$  to  $150^\circ\text{C}$ ,  $T_J \leq T_{J(\text{max})}$ , over full range of AG, unless otherwise noted

Characteristic	Symbol	Test Conditions	Min.	Typ. <sup>1</sup>	Max.	Units		
<b>SWITCHPOINT CHARACTERISTICS</b>								
Tooth Speed	S	Tooth frequency, target generating sinusoidal signal	0	–	8	kHz		
Bandwidth	BW	Corresponds to output switching frequency – 3 dB	–	40	–	kHz		
Operate	$B_{OP}$	ATS673	% of peak-to-peak, referenced to tooth signal,		–	40	%	
		ATS674	AG < $AG_{(\text{Max})}$		–	30	%	
Release	$B_{RP}$	ATS673	% of peak-to-peak, referenced to tooth signal,		–	50	%	
		ATS674	AG < $AG_{(\text{Max})}$		–	40	%	
<b>CALIBRATION CHARACTERISTICS<sup>4</sup></b>								
Initial Calibration	$Cal_{IC}$	Quantity of rising edges required to complete edge detection calibration	–	–	3	edges		
AGC Disable	$Cal_{AGC}$	Quantity of rising edges required to complete Automatic Gain Control calibration	–	–	3	edges		
Calibration Update	$Cal_{UPD}$	Quantity of rising edges required to update edge detection calibration while running after initial calibration	–	Continuous	–	edges		
<b>PERFORMANCE CHARACTERISTICS<sup>3</sup></b>								
TPOS Air Gap Range <sup>5</sup>	$AG_{TPOS}$	TPOS functionality guaranteed	0.5	–	2.5	mm		
Operational Air Gap Range	AG	TPOS guaranteed, output switching, running mode	0.5	–	2.5	mm		
Extended Minimum Air Gap <sup>6</sup>	$AG_{EXTMIN}$	Output switching, running mode; valleys may be detected as teeth in this range	–	–	0.5	mm		
Extended Maximum Air Gap <sup>7</sup>	$AG_{EXTMAX}$	Output switching, running mode; teeth may be detected as valleys in this range	2.5	–	5	mm		
Relative Timing Accuracy <sup>4,8</sup>	$Err_{ICREL}$	ATS673	During initial calibration; rising or falling edges, gear speed = 1000 rpm, target eccentricity		–	3	deg	
		ATS674	< 0.1 mm		–	3	deg	
	$Err_{RELR}$	ATS673	Rising edges; after initial calibration, gear speed = 1000 rpm, target eccentricity < 0.1 mm		–	0.5	0.8	deg
		ATS674			–	0.4	0.8	deg
	$Err_{RELF}$	ATS673	Falling edges; after initial calibration, gear speed = 1000 rpm, target eccentricity < 0.1 mm		–	0.8	1.2	deg
		ATS674			–	0.6	1.2	deg
Phase Delay <sup>9</sup>	$\Delta Err_{SREL}$	After initial calibration, AG = 1.5 mm, $T_A = 25^\circ\text{C}$	–	$1.6 \times 10^{-4}$	–	deg/rpm		

<sup>1</sup>Typical values are taken at  $V_{CC} = 12\text{ V}$  and  $T_A = 25^\circ\text{C}$ .

<sup>2</sup> $I_{ZSupply(\text{Max})}$  is equivalent to  $I_{CCON(\text{Max})} + 3\text{ mA}$ .

<sup>3</sup>Using reference target 8X.

<sup>4</sup>The term *edge* refers to a mechanical edge, such as the side of a gear tooth, passing under the device. Rising edge: from valley to approaching tooth. Falling edge: from tooth to approaching valley.

<sup>5</sup>The TPOS Air Gap Range is the range of installation air gaps within which the TPOS (True Power-On State) function is guaranteed to correctly detect a tooth when powered-on over a tooth and correctly detecting a valley when powered-on over a valley, using reference target 8X or equivalent, as specified in the Target/Gear Parameters for Correct TPOS Operation section in this document.

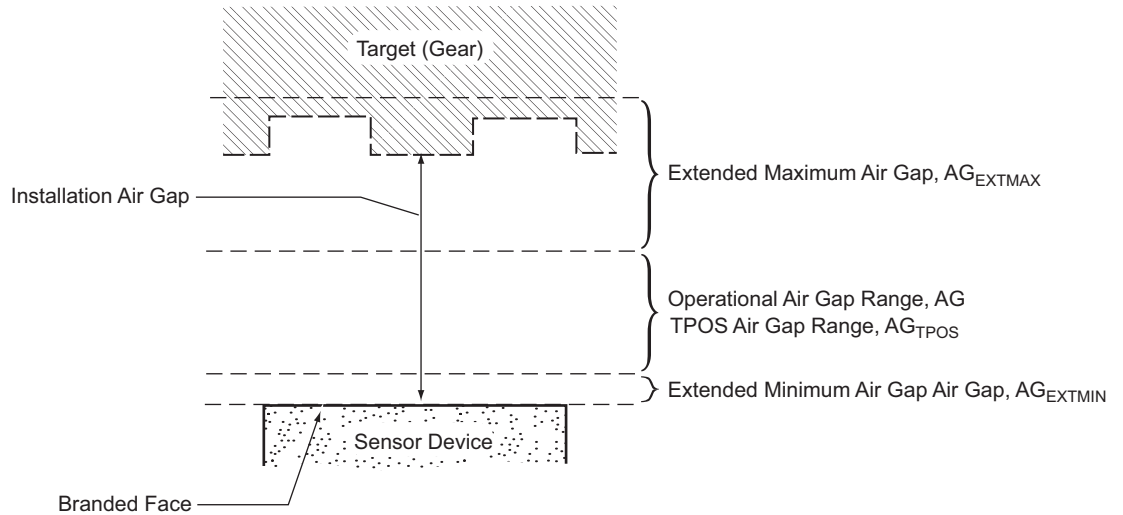
<sup>6</sup>The Extended Minimum Air Gap is a range of installation air gaps, smaller than  $AG_{(\text{Min})}$ , within which the the device will accurately detect target features but TPOS is NOT guaranteed to be fully accurate, possibly evaluating the initial valley as a tooth.

<sup>7</sup>The Extended Maximum Air Gap is an extended range of installation air gaps, greater than  $AG_{(\text{Max})}$ , within which the the device will accurately detect target features but TPOS is not guaranteed to be fully accurate, possibly evaluating the initial tooth as a valley.

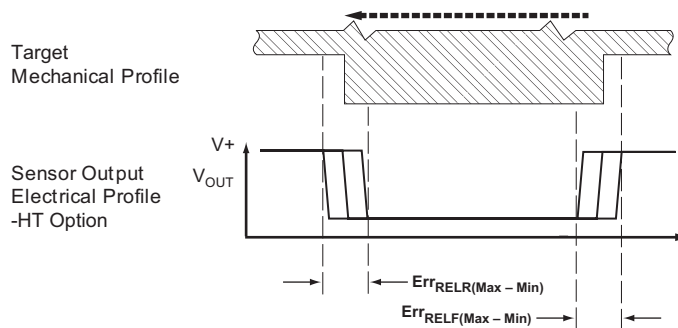
<sup>8</sup>Relative Timing Accuracy is the change in edge position before the resulting change in device output; for a single device, over the full Operational Air Gap Range, AG, and Operating Ambient Temperature,  $T_A$ , range.

<sup>9</sup>Phase Delay is the change in edge position at detection, through the full operational Tooth Speed, S, range for a single device, and at a single ambient temperature,  $T_A$ , and installation air gap, AG.

**Air Gap Comparisons**



**Relative Timing Accuracy**



Reference Target (Gear) Information

REFERENCE TARGET 8X

Characteristic	Symbol	Test Conditions	Typ.	Units	Symbol Key
Outside Diameter	$D_o$	Outside diameter of target	120	mm	
Face Width	$F$	Breadth of tooth, with respect to sensor	6	mm	
Circular Tooth Length	$t$	Length of tooth, with respect to sensor; measured at $D_o$	23.6	mm	
Circular Valley Length	$t_v$	Length of valley, with respect to sensor; measured at $D_o$	23.6	mm	
Tooth Whole Depth	$h_t$		5	mm	
Material		CRS 1018	-	-	

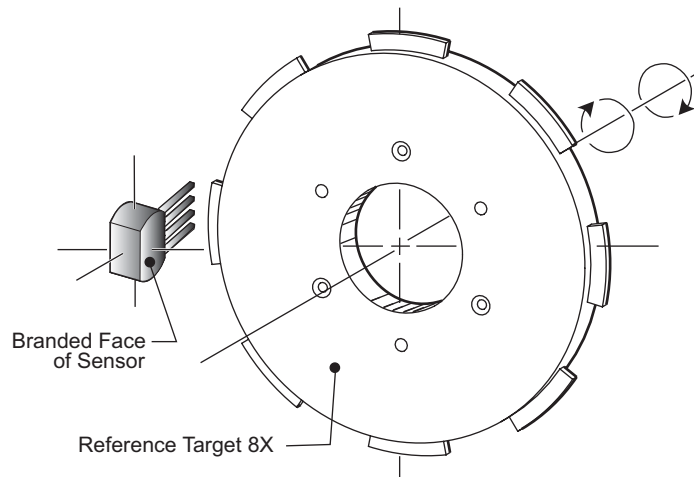


Figure 1. Configuration with Reference Target

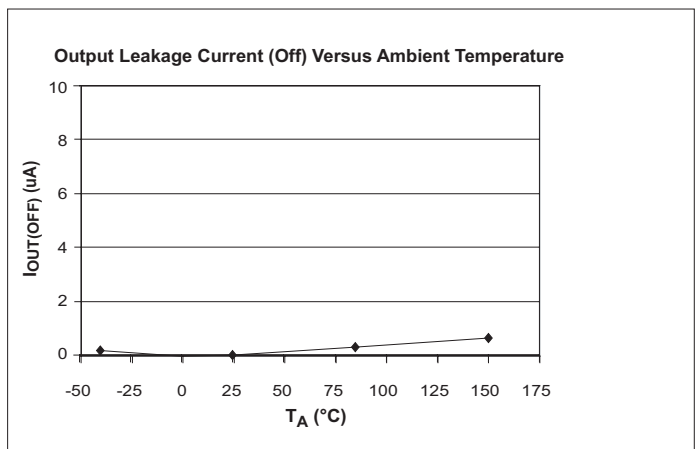
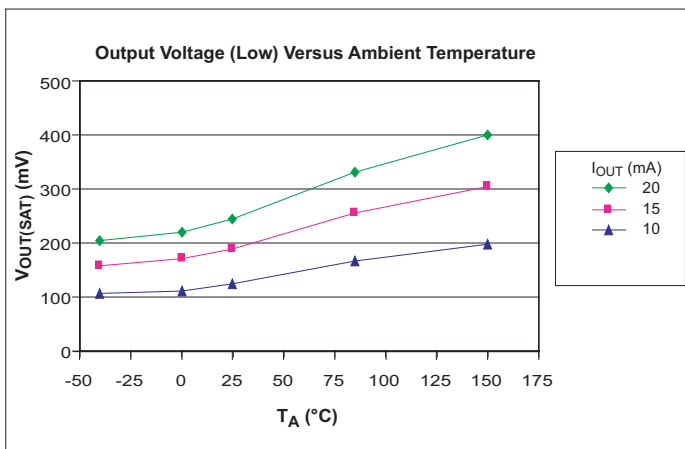
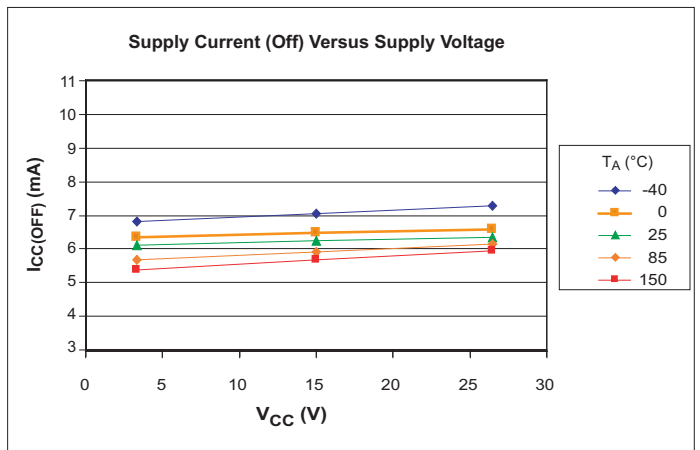
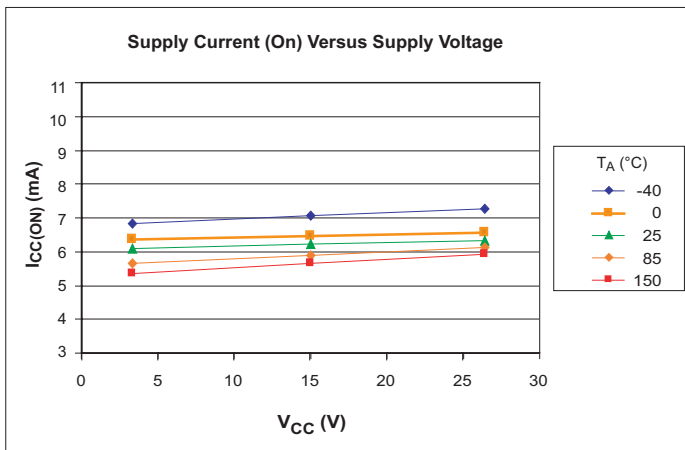
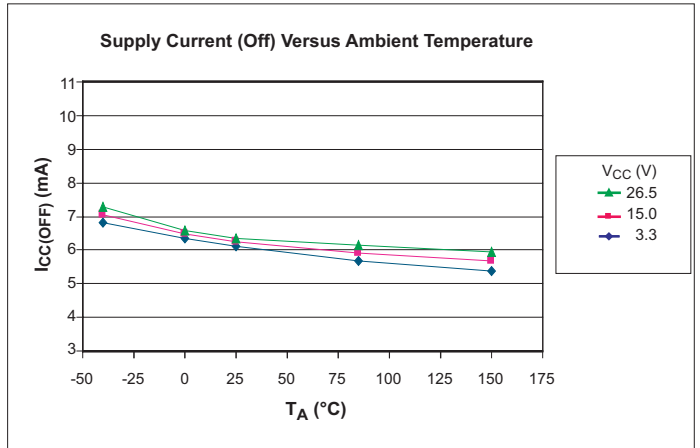
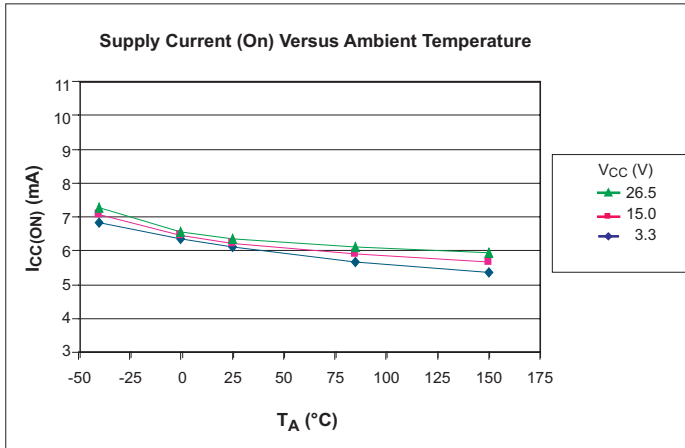
**Target/Gear Parameters for Correct TPOS Operation**

For TPOS to function as specified, the target must generate a minimum of 120 G difference between the magnetic field over a tooth and the field over a valley, at the maximum installation air gap. A target complying with the material and dimensions cited for the reference target 8X, generates the required 120 G differential.

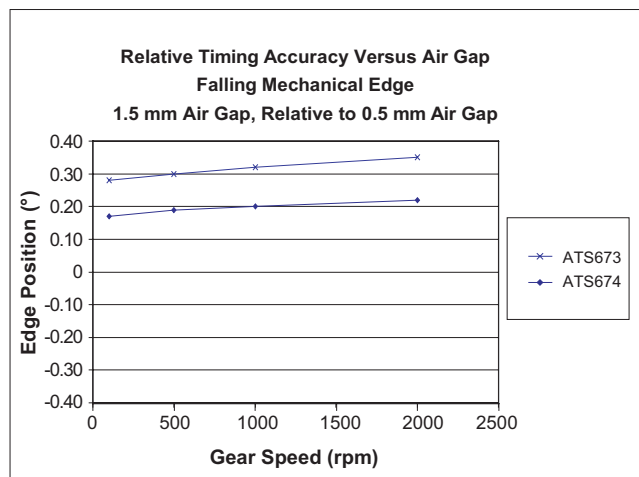
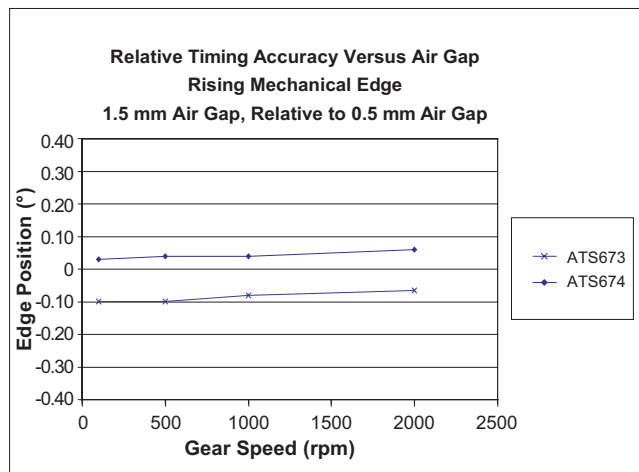
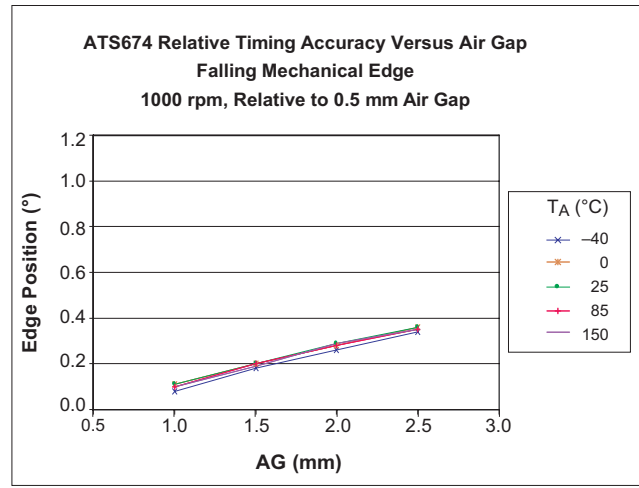
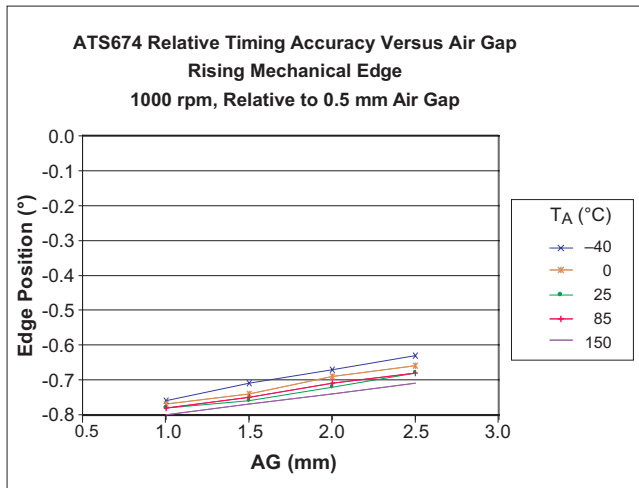
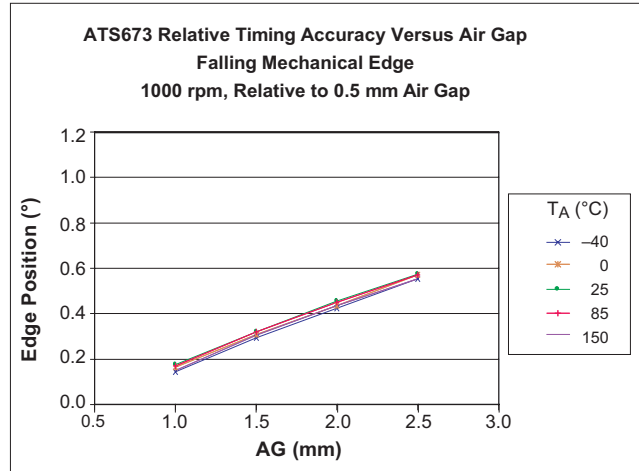
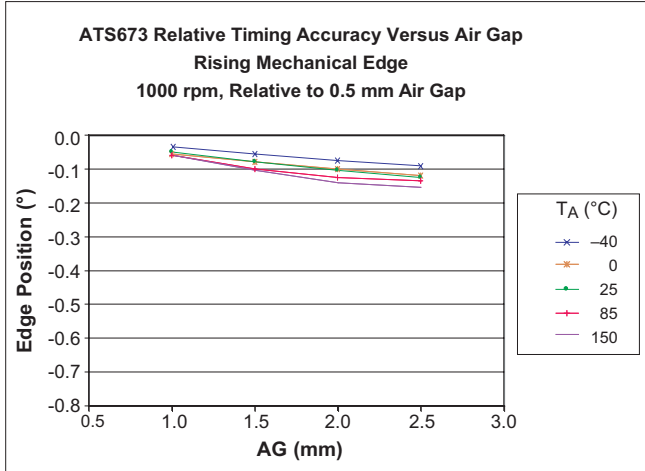
The following recommendations should be followed in the design and specification of targets:

- Tooth width,  $t \geq 5$  mm
- Valley width,  $t_v > 13$  mm
- Valley depth,  $h_t > 5$  mm
- Tooth thickness,  $F \geq 5$  mm

Characteristic Data: Electrical



Characteristic Data: Relative Timing Accuracy





**Operational Description**

**Assembly Description**

The ATS673 and ATS674 true zero-speed gear tooth sensors have a Hall IC-magnet configuration that is fully optimized to provide digital detection of gear tooth edges. This sensor is integrally molded into a plastic body that has been optimized for size, ease of assembly, and manufacturability. High operating temperature materials are used in all aspects of construction.

**Sensing Technology**

The gear tooth sensor contains a single-chip Hall effect sensor IC, a 4-pin leadframe and a specially designed rare-earth magnet. The Hall IC supports a Hall element that measures the magnetic gradient created by the passing of a ferrous object. This

is illustrated in figure 2. The difference in the magnetic gradients created by teeth and valleys allows the devices to generate a digital output signal.

**Output**

After proper power is applied to the devices, they are then capable of providing digital information that is representative of the profile of a rotating gear, as illustrated in figure 3. No additional optimization is needed and minimal processing circuitry is required. This ease of use reduces design time and incremental assembly costs for most applications.

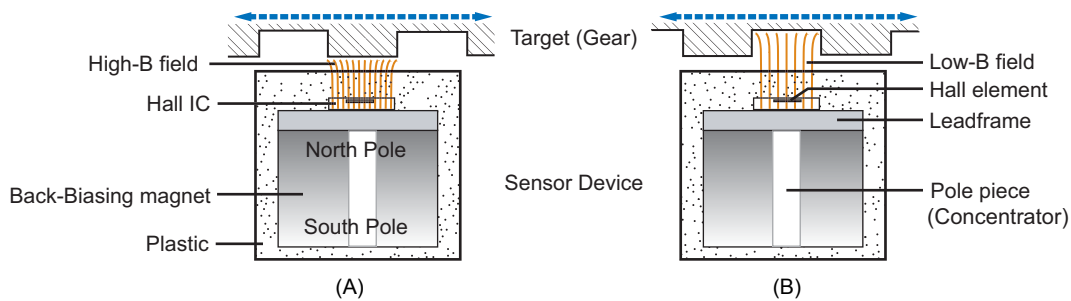


Figure 2. Device Cross Section. Motion of the target is detected by the Hall element mounted on the Hall IC. Panel A, the presence of a tooth feature on the target is distinguished by a high magnetic flux density, B. Panel B, the presence of a valley feature is distinguished by its low magnetic flux density.

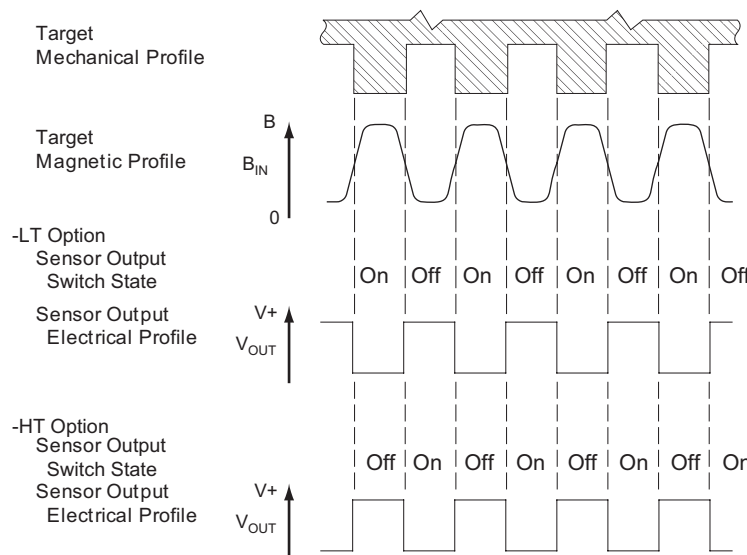


Figure 3. The magnetic profile reflects the geometry of the target, allowing the device to present an accurate digital output response.

**TPOS (True Power-On State) Operation**

Under specified operating conditions, the devices are guaranteed to attain a specified output voltage polarity at power-on, in relation to the target feature nearest the device at that time. Both devices offer the options of either high or low polarity over initial tooth or valley. This polarity also applies throughout device operation.

**Start-Up Detection**

These devices provide an output polarity transition at the first mechanical edge after power-on.

**Undervoltage Lockout**

When the supply voltage falls below the undervoltage lockout level,  $V_{CCUV}$ , the device switches to the OFF state. The device remains in that state until the voltage level is restored to the  $V_{CC}$  operating range. Changes in the target magnetic profile have no effect until voltage is restored. This prevents false signals caused by undervoltage conditions from propagating to the output of the sensor.

**Power Supply Protection**

The ATS673 and ATS674 contain an on-chip regulator and can operate over a wide range of supply voltage levels. For applications using an unregulated power supply, transient protection must be added externally. For applications using a regulated supply line, EMI and RFI protection may still be required. The circuit shown in figure 5 is the basic configuration required for proper device operation. Contact Allegro field applications engineering for information on the circuitry required for compliance to various EMC specifications.

**Internal Electronics**

These devices contain a self-calibrating Hall effect IC that provides a Hall element, a temperature compensated amplifier, and offset cancellation circuitry. The IC also contains a voltage regulator that provides supply noise rejection over the operating voltage range. The Hall transducers and the electronics are integrated on the same silicon substrate by a proprietary BiCMOS process. Changes in temperature do not greatly affect this device due to the stable amplifier design and the offset rejection circuitry.

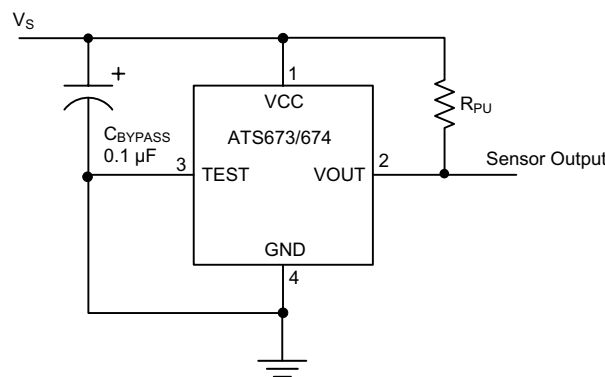


Figure 5. Power Supply Protection Typical Circuit

**AGC (Automatic Gain Control)**

The AGC feature is implemented by a unique patented self-calibrating circuitry. After each power-on, the devices measure the peak-to-peak magnetic signal. The gain of the sensor is then

adjusted, keeping the internal signal amplitude constant over the air gap range of the device. This feature ensures that operational characteristics are isolated from the effects of changes in AG. The effect of AGC is shown in figure 7.

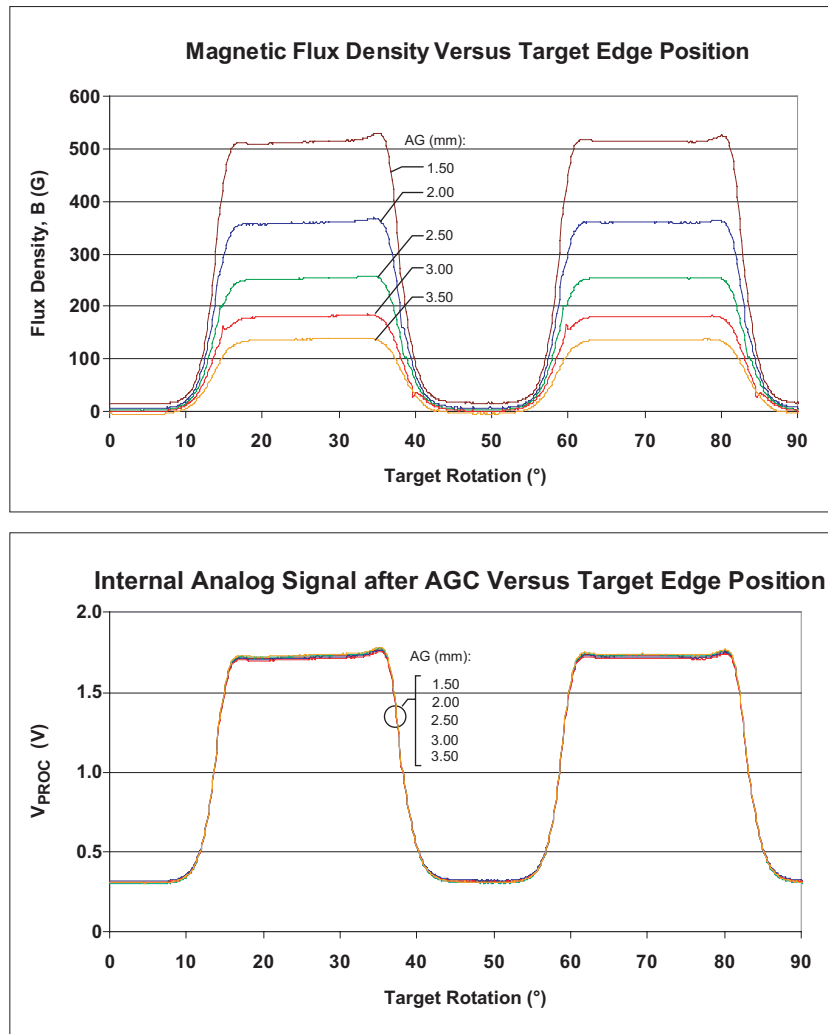


Figure 7. Effect of AGC. The upper panel shows the magnetic gradient detected at the Hall element, with no amplification. The lower panel displays the corresponding internal processed signal,  $V_{PROC}$ . This normalized electrical signal allows optimal performance by the rest of the circuits that reference this signal.

**Switchpoints**

Switchpoints in the ATS673 and ATS674 are established dynamically as a percentage of the amplitude of the signal,  $V_{PROC}$ , after normalization with AGC. Two DACs track the peaks of  $V_{PROC}$  (see the *Update* subsection).

The switching thresholds are established at fixed percentages of the values held in the two DACs. The value of the thresholds has been carefully selected, where the signal is steepest and least affected by air gap variation, thus providing the most accurate and consistent switching.

The low hysteresis, 10%, provides high performance over various air gaps while maintaining immunity to false switching on noise, vibration, backlash, or other transient events.

Figure 8 graphically demonstrates the establishment of the switching threshold levels. Because the thresholds are established dynamically as a percentage of the peak-to-peak signal, the effect of a baseline shift is minimized.

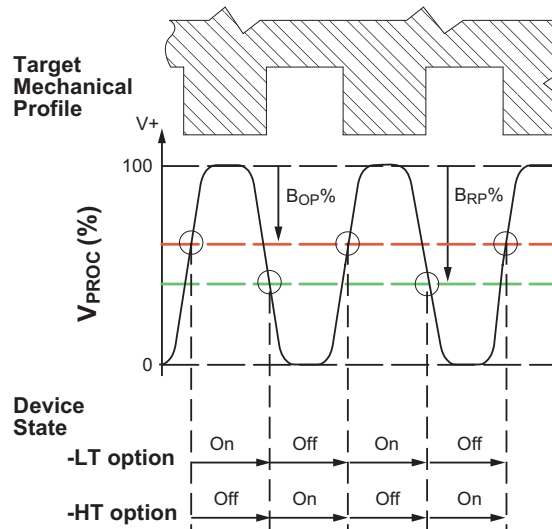


Figure 8. Switchpoint Relationship to Thresholds. The device switches when  $V_{PROC}$  passes a threshold level,  $B_{OP}$  or  $B_{RP}$ , while changing in the corresponding direction: increasing for a  $B_{OP}$  switchpoint, and decreasing for a  $B_{RP}$  switchpoint.

**Update**

The ATS673 and ATS674 incorporate an algorithm that continuously monitors the system and updates the switching thresholds accordingly. The switchpoint for each transition is determined by the previous two transitions. Because variations are tracked

in real time, the sensor has high immunity to target run-out and retains excellent accuracy and functionality in the presence of both run-out and transient mechanical events. Figure 9 shows how the devices use historical data to provide the switching thresholds for a given edge.

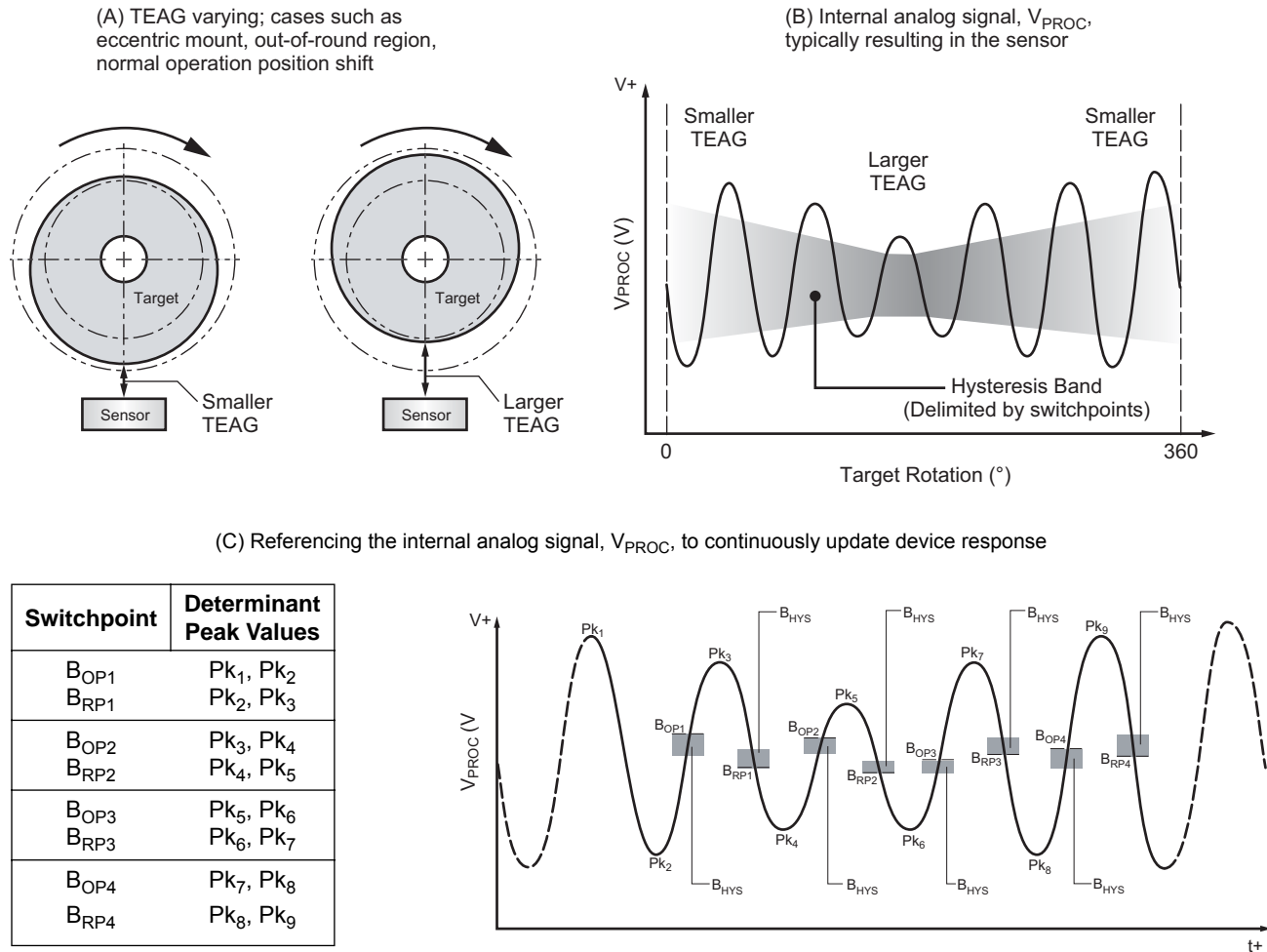


Figure 9. The Continuous Update algorithm allows the Allegro sensor to immediately interpret and adapt to significant variances in the magnetic field generated by the target as a result of eccentric mounting of the target, out-of-round target shape, elevation due to lubricant build-up in journal gears, and similar dynamic application problems that affect the TEAG (Total Effective Air Gap). The algorithm is used to dynamically establish and subsequently update the device switchpoints ( $B_{OP}$  and  $B_{RP}$ ). The hysteresis,  $B_{HYS(\#x)}$ , at each target feature configuration results from this recalibration, ensuring that it remains properly proportioned and centered within the peak-to-peak range of the internal analog signal,  $V_{PROC}$ .

As shown in panel A, the variance in the target position results in a change in the TEAG. This affects the sensor as a varying magnetic field, which results in proportional changes in the internal analog signal,  $V_{PROC}$ , shown in panel B. The Continuous Update algorithm is used to establish accurate switchpoints based on the fluctuation of  $V_{PROC}$ , as shown in panel C.

Sensor and Target Evaluation

**Magnetic Profile**

In order to establish the proper operating specification for a particular sensor device and target system, a systematic evaluation of the magnetic circuit should be performed. The first step is the generation of a magnetic map of the target. By using a calibrated device, a magnetic profile of the system is made. Figure 10 is a magnetic map of the 8X reference target.

A pair of curves can be derived from this map data, and be used to describe the tooth and valley magnetic field strength, B, versus the size of the air gap, AG. This allows determination of the minimum amount of magnetic flux density that guarantees operation of the sensor, so the system designer can determine the maximum allowable AG for the sensor and target system. One can also determine the TPOS air gap capabilities of the sensor by comparing the minimum tooth signal to the maximum valley signal.

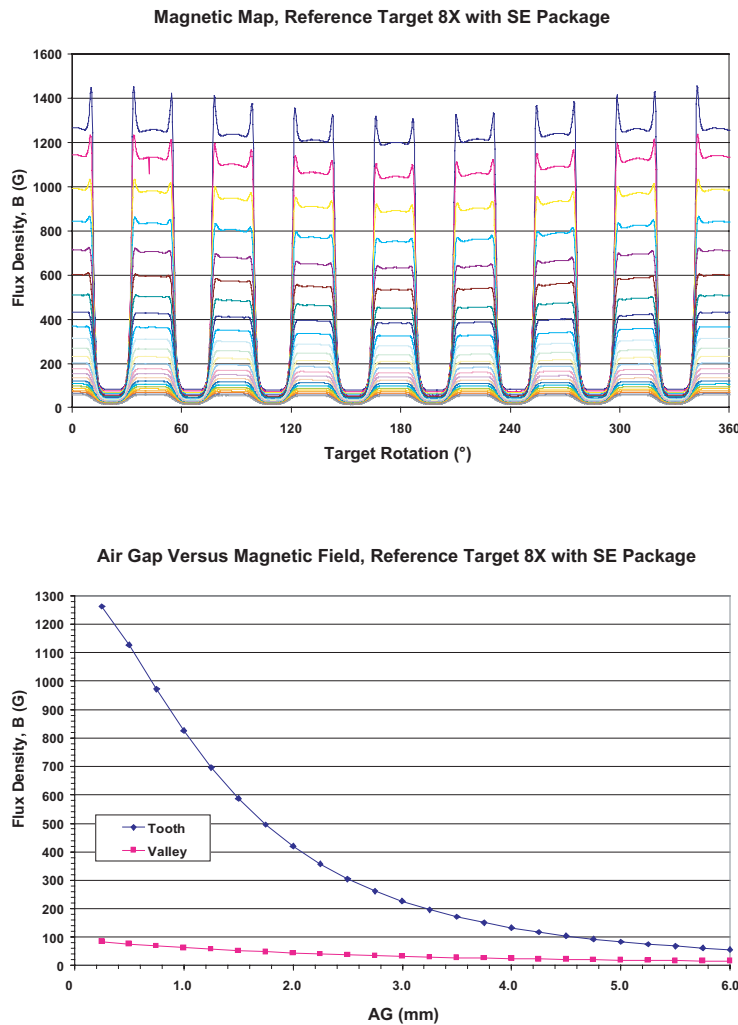


Figure 10. Magnetic Data for the 8X Reference Target and SE package.

**Accuracy**

While the update algorithm will allow the sensor devices to adapt to typical air gap variations, major changes in air gap can adversely affect switching performance. When characterizing sensor performance over a significant air gap range, be sure to

repower the device at each test at different air gaps. This ensures that self-calibration occurs for each installation condition. See the *Operating Characteristics* table and the charts in the *Characteristic Data: Relative Timing Accuracy* section for performance information.

**Sensor Evaluation: EMC**

Characterization Only

<b>Test Name*</b>	<b>Reference Specification</b>
ESD – Human Body Model	AEC-Q100-002
ESD – Machine Model	AEC-Q100-003
Conducted Transients	ISO 7637-1
Direct RF Injection	ISO 11452-7
Bulk Current Injection	ISO 11452-4
TEM Cell	ISO 11452-3

\*Please contact Allegro for EMC performance

**Related Documents**

Documents that can be found on the Allegros web site, :  
[www.allegromicro.com](http://www.allegromicro.com):

- Definition of Terms (Pub 26004)
- Hall-Effect Devices: Soldering, Gluing, Potting, Encapsulating, and Lead forming (AN27703.1)
- Storage of Semiconductor Devices (Pub 26011)
- Hall Effect Applications Guide (Pub 27701)
- Applications Note: Back-Biased Packaging Advances (SE, SG & SH versus SA & SB)



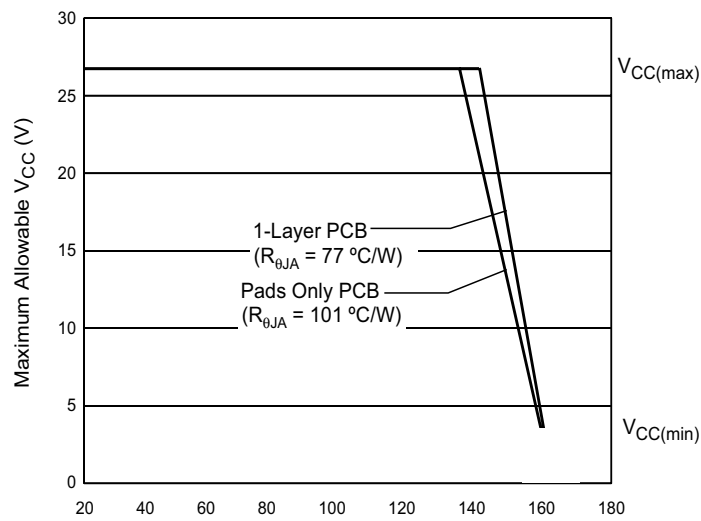
**Power Derating**

**THERMAL CHARACTERISTICS may require derating at maximum conditions, see application information**

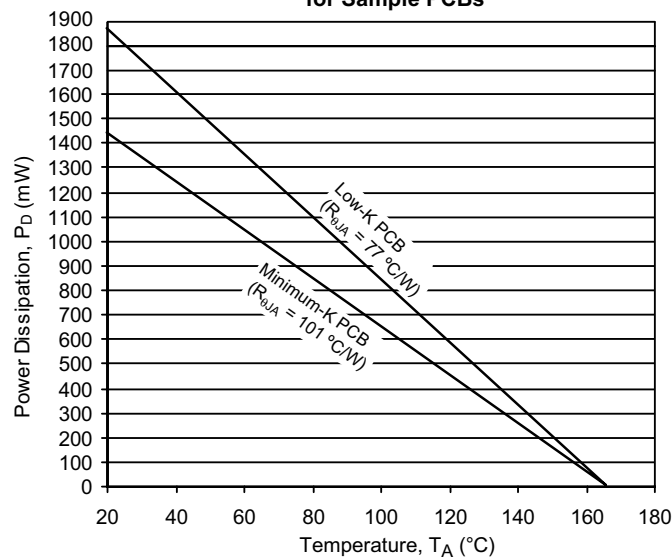
Characteristic	Symbol	Test Conditions*	Value	Units
Package Thermal Resistance	$R_{\theta JA}$	1-layer PCB with copper limited to solder pads	101	$^{\circ}\text{C}/\text{W}$
		1-layer PCB with copper limited to solder pads and 3.57 in. <sup>2</sup> (23.03 cm <sup>2</sup> ) of copper area each side	77	$^{\circ}\text{C}/\text{W}$

\*Additional information is available on the Allegro Web site.

**Power Derating Curve**



**Power Dissipation Versus Ambient for Sample PCBs**





The device must be operated below the maximum junction temperature of the device,  $T_{J(max)}$ . Under certain combinations of peak conditions, reliable operation may require derating supplied power or improving the heat dissipation properties of the application. This section presents a procedure for correlating factors affecting operating  $T_J$ . (Thermal data is also available on the Allegro MicroSystems Web site.)

The Package Thermal Resistance,  $R_{\theta JA}$ , is a figure of merit summarizing the ability of the application and the device to dissipate heat from the junction (die), through all paths to the ambient air. Its primary component is the Effective Thermal Conductivity,  $K$ , of the printed circuit board, including adjacent devices and traces. Radiation from the die through the device case,  $R_{\theta JC}$ , is relatively small component of  $R_{\theta JA}$ . Ambient air temperature,  $T_A$ , and air motion are significant external factors, damped by overmolding.

The effect of varying power levels (Power Dissipation,  $P_D$ ), can be estimated. The following formulas represent the fundamental relationships used to estimate  $T_J$ , at  $P_D$ .

$$P_D = V_{IN} \times I_{IN} \quad (1)$$

$$\Delta T = P_D \times R_{\theta JA} \quad (2)$$

$$T_J = T_A + \Delta T \quad (3)$$

For example, given common conditions such as:  $T_A = 25^\circ\text{C}$ ,  $V_{IN} = 12\text{ V}$ ,  $I_{IN} = 4\text{ mA}$ , and  $R_{\theta JA} = 140\text{ }^\circ\text{C/W}$ , then:

$$P_D = V_{IN} \times I_{IN} = 12\text{ V} \times 4\text{ mA} = 48\text{ mW}$$

$$\Delta T = P_D \times R_{\theta JA} = 48\text{ mW} \times 140\text{ }^\circ\text{C/W} = 7^\circ\text{C}$$

$$T_J = T_A + \Delta T = 25^\circ\text{C} + 7^\circ\text{C} = 32^\circ\text{C}$$

A worst-case estimate,  $P_{D(max)}$ , represents the maximum allowable power level, without exceeding  $T_{J(max)}$ , at a selected  $R_{\theta JA}$  and  $T_A$ .

*Example:* Reliability for  $V_{CC}$  at  $T_A = 150^\circ\text{C}$ , package SE, using minimum-K PCB.

Observe the worst-case ratings for the device, specifically:  $R_{\theta JA} = 101^\circ\text{C/W}$ ,  $T_{J(max)} = 165^\circ\text{C}$ ,  $V_{CC(max)} = 26.5\text{ V}$ , and  $I_{CC(max)} = 11\text{ mA}$ . Note that  $I_{CC(max)}$  at  $T_A = 150^\circ\text{C}$  is lower than the  $I_{CC(max)}$  at  $T_A = 25^\circ\text{C}$  given in the Operating Characteristics table.

Calculate the maximum allowable power level,  $P_{D(max)}$ . First, invert equation 3:

$$\Delta T_{max} = T_{J(max)} - T_A = 165^\circ\text{C} - 150^\circ\text{C} = 15^\circ\text{C}$$

This provides the allowable increase to  $T_J$  resulting from internal power dissipation. Then, invert equation 2:

$$P_{D(max)} = \Delta T_{max} \div R_{\theta JA} = 15^\circ\text{C} \div 101\text{ }^\circ\text{C/W} = 91\text{ mW}$$

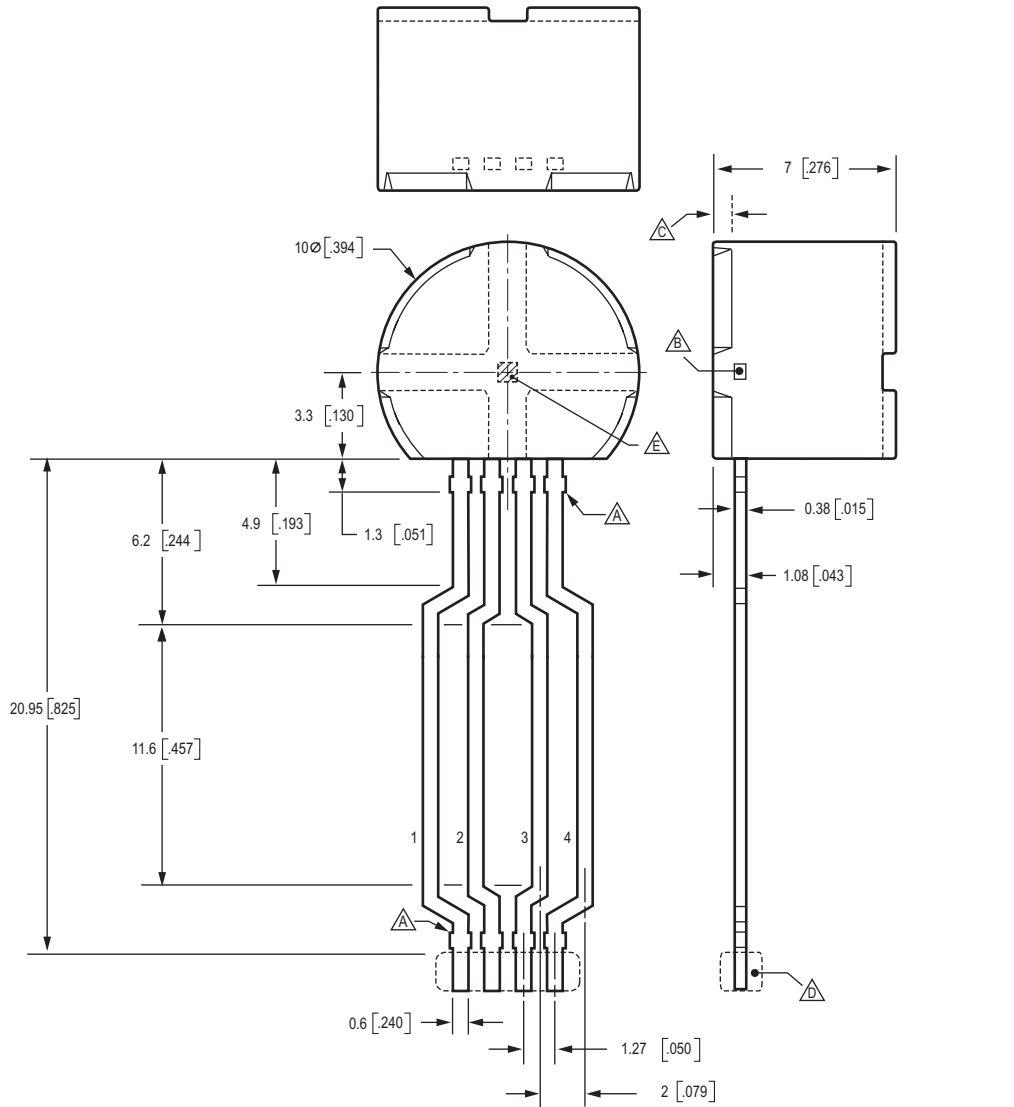
Finally, invert equation 1 with respect to voltage:

$$V_{CC(est)} = P_{D(max)} \div I_{CC(max)} = 91\text{ mW} \div 11\text{ mA} = 8.3\text{ V}$$

The result indicates that, at  $T_A$ , the application and device can dissipate adequate amounts of heat at voltages  $\leq V_{CC(est)}$ .

Compare  $V_{CC(est)}$  to  $V_{CC(max)}$ . If  $V_{CC(est)} \leq V_{CC(max)}$ , then reliable operation between  $V_{CC(est)}$  and  $V_{CC(max)}$  requires enhanced  $R_{\theta JA}$ . If  $V_{CC(est)} \geq V_{CC(max)}$ , then operation between  $V_{CC(est)}$  and  $V_{CC(max)}$  is reliable under these conditions.

**Package SE, 4-Pin SIP**



Preliminary dimensions, for reference only  
 Untoleranced dimensions are nominal.  
 Dimensions in millimeters  
 U.S. Customary dimensions (in.) in brackets, for reference only  
 Dimensions exclusive of mold flash, burrs, and dambar protrusions  
 Exact case and lead configuration at supplier discretion within limits shown

- △ Dambar removal protrusion (16X)
- △ Metallic protrusion, electrically connected to pin 4 and substrate (both sides)
- △ Active Area Depth, 0.43 mm [0.017]
- △ Thermoplastic Molded Lead Bar for alignment during shipment
- △ Hall element (not to scale)

*The products described herein are manufactured under one or more of the following U.S. patents: 5,045,920; 5,264,783; 5,442,283; 5,389,889; 5,581,179; 5,517,112; 5,619,137; 5,621,319; 5,650,719; 5,686,894; 5,694,038; 5,729,130; 5,917,320; 6,297,627; 6,525,531; and other patents pending.*

*Allegro MicroSystems, Inc. reserves the right to make, from time to time, such departures from the detail specifications as may be required to permit improvements in the performance, reliability, or manufacturability of its products. Before placing an order, the user is cautioned to verify that the information being relied upon is current.*

*Allegro products are not authorized for use as critical components in life-support devices or systems without express written approval.*

*The information included herein is believed to be accurate and reliable. However, Allegro MicroSystems, Inc. assumes no responsibility for its use; nor for any infringement of patents or other rights of third parties which may result from its use.*

*Copyright © 2005, 2006 Allegro MicroSystems, Inc.*

